Heat Mass Transfer (2009) 45:1047–1059
DOI 10.1007/s00231-009-0476-y

ORIGINAL

Analysis of heat conduction in a disk brake system

Faramarz Talati · Salman Jalalifar

Received: 3 July 2008 / Accepted: 5 January 2009 / Published online: 27 January 2009

Abstract In this paper, the governing heat equations for the disk and the pad are extracted in the form of transient heat equations with heat generation that is dependant to time and space. In the derivation of the heat equations, parameters such as the duration of braking, vehicle velocity, geometries and the dimensions of the brake components, materials of the disk brake rotor and the pad and contact pressure distribution have been taken into account. The problem is solved analytically using Green's function approach. It is concluded that the heat generated due to friction between the disk and the pad should be ideally dissipated to the environment to avoid decreasing the friction coefficient between the disk and the pad and to avoid the temperature rise of various brake components and brake fluid vaporization due to excessive heating.

List of symbols

c	Specific heat (J kg^{-1} K^{-1})
d_1	Pad thickness (m)
d_2	Disk thickness (m)
$\mathrm{d}\dot{E}$	Thermal energy per unit time (W)
$\mathrm{d}P$	Friction power (W)
E_c	Kinetic energy (J)
F_f	Friction force (N)
h	Heat transfer coefficient (W m^{-2} K^{-1})
$J_0(\cdot)$	Bessel's function of the first kind
k	Thermal conductivity (W m^{-1} K^{-1})
M	Total vehicle mass (kg)
m	Mass of the vehicle distributed on the front axle (kg)
$p_{\max}$	Maximum pressure in the pad (N m^{-2})
p	Pressure at radial distance r (N m^{-2})
$\dot{q}$	Heat flux density (W m^{-2})
q_0	Heat flux density at time $t = 0$ (W m^{-2})
r	Space variable in radial distance (m)
r'	Dummy space variable in radial distance (m)
r_1	Inner disk radius (m)
r_2	Inner pad radius (m)
r_3	Outer radius of the disk and the pad (m)
S	Frictional surface (m^2)
t	Time (s)
t_b	Braking time (s)
T_0	Initial temperature (K)
T_∞	Ambient temperature (K)
$Y_0(\cdot)$	Bessel's function of the second kind
V	Instantaneous velocity of the vehicle (m s^{-1})
V_0	Initial velocity of the vehicle (m s^{-1})
z	Space variable in axial direction (m)
z'	Dummy space variable in axial direction (m)

Greek symbols

α	Thermal diffusivity (m s^{-2})
σ	Heat partition coefficient, dimensionless
ϕ_0	Pad contact angle (Rad)
ξ	Thermal effusivity (Jm^2 K^{-1} s$^{-0.5}$)
ρ	Mass density (kg m^{-3})
μ	Coefficient of friction, dimensionless
ω	Instantaneous angular velocity of the disk (s^{-1})
ω_0	Initial angular velocity of the disk (s^{-1})
τ	Dummy variable for time (s)

F. Talati · S. Jalalifar (✉)
Faculty of Mechanical Engineering, University of Tabriz, Tabriz, Iran
e-mail: S.jalalifar@gmail.com

F. Talati
e-mail: talati@tabrizu.ac.ir

Subscripts

d Disk
p Pad

1 Introduction

Recently, disk brakes have been widely used in light vehicles. Proper performance of a vehicle brake system is one of its advantages. Long repetitive braking leads to temperature rise of various brake components of the vehicle that reduces the performance of the brake system.

Long repetitive braking, such as one which occurs during a mountain descent, will result in a brake fluid temperature rise and may cause brake fluid vaporization. This may be a concern particularly for passenger cars equipped with aluminum calipers and with a limited air flow to the wheel brake systems. Braking performance of a vehicle can be significantly affected by the temperature rise in the brake components. High temperature during braking may cause brake fade, premature wear, brake fluid vaporization, bearing failure, thermal cracks, and thermally excited vibration. Therefore, it is important to predict the temperature rise of a given brake system and assess its thermal performance in the early design stage. Recently, brake fluid vaporization has been suspected as a possible cause of some collisions and a proper inspection procedure has been recommended [1, 2].

Disk brakes are exposed to large thermal stresses during routine braking and extraordinary thermal stresses during hard braking. High-g decelerations typical of passenger vehicles are known to generate temperatures as high as 900°C in a fraction of a second. These large temperature excursions have two possible outcomes: thermal shock that generates surface cracks; and/or large amounts of plastic deformation in the brake rotor. In the absence of thermal shock, a relatively small number of high-g braking cycles are found to generate macroscopic cracks running through the rotor thickness and along the radius of the disk brake [3].

Heat generation due to friction in the sliding contact of two bodies influences friction and wear characteristics of brake systems. We note that numerous experimental evidences suggest that the contact area is generally circular, e.g. tread broke railway wheels exhibit circular thermally affected zones on the surface [4].

According to Ostermeyer [5], the contact area in brake systems shows characteristic structures. With respect to wear, equilibrium of flow of growing and destruction of hard patches is to be found on the contact surface. These patches modulate the friction coefficient of the brake system. Dealing with this principal wear mechanism of brake pads the dynamic friction coefficient describes the stationary and transient friction behavior of brake pads. For instance the fading effect is the result of a temporary higher destruction rate than the grow rate, when normal force and velocity get high, up to that point, where the equilibrium of flow of power is reached again on a lower level.

Gao and Lin [6] have presented an analytical model for the determination of the contact temperature distribution on the working surface of a brake. To consider the effects of the moving heat source (the pad) with relative sliding speed variation, a transient finite element technique is used to characterize the temperature fields of the solid rotor with appropriate thermal boundary conditions. Numerical results shows that the operating characteristics of the brake exert an essentially influence on the surface temperature distribution and the maximal contact temperature.

Dufrénoy [7] proposed a macrostructural model of the thermomechanical behavior of the disk brake, taking into account the real three-dimensional geometry of the disk–pad couple. Contact surface variations, distortions and wear are taken into account. Real body geometry and thermoelastoplastic modeling of the disk material are specially introduced. Such a model aims to give predictions of the thermal gradients varying with time and of the thermomechanical response of the components. Predictions of the temperature distributions are compared with experimental measurements obtained by thermographs and thermocouples. Such a model seems to be a suitable base for the study of the thermal dissipation and the thermomechanical behavior and for the introduction of local friction effects.

Formation of hot spots as well as non-uniform distribution of the contact pressure is an unwanted effect emerging in disk brakes in the course of braking or during engagement of a transmission clutch. If the sliding velocity is high enough, this effect can become unstable and can result in disk material damage, frictional vibration, wear, etc. [8].

Naji et al. [9] presented a mathematical model to describe the thermal behavior of a brake system which consists of the shoe and the drum. The model is solved analytically using Green's function method for any type of the stopping braking action. The thermal behavior is investigated for three specified braking actions which were the impulse, the unit step and trigonometric stopping actions.

Thermal response of disk brake systems to different materials used for the disk–pad couple has been studied in many researches [10–17].

Aerodynamic cooling of high performance disk brake systems is investigated by many researchers [18–20].

This paper presents a mathematical model for describing the thermal behavior of a disk brake system in a vehicle.

The time dependant heat equation is extracted from the energy balance for the brake rotor and the pad. In derivation of the equations, different aspects with the assumption of constant deceleration braking action have been considered including different pressure distributions. Appropriate boundary conditions have been used to solve the governing equations using Green's function approach. Effects of various design parameters, geometry and operating conditions are taken into account.

2 Formulation of the problem

Figure 1 shows the disk brake system of a car and pad that is separated from wheel assembly to better show the disk and the pad in sliding contact. As it can be seen, typical disk brake system and caliper assembly of a solid disk brake rotor is completely noticeable. Figure 2 shows schematic form of the disk and the pad in sliding contact.

2.1 Models of heat dissipation in disk brakes

2.1.1 Macroscopic model

Brakes are essentially a mechanism to change the energy types. When a car is moving with speed, it has *kinetic energy*. Applying the brakes, the pads or shoes that press against the brake drum or rotor convert this energy into *thermal energy*. The cooling of the brakes dissipates the heat and the vehicle slows down. This is all to do with *the first law of thermodynamics*, sometimes known as the *law of conservation of energy* that states that energy cannot be created nor destroyed; it can only be converted from one form to another. In the case of brakes, it is converted from kinetic energy to thermal energy:

Fig. 1 Disk brake rotor, pad, and caliper assembly

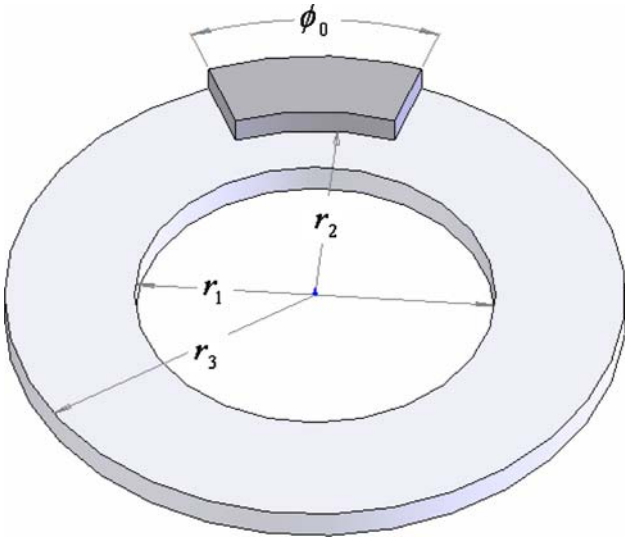

Fig. 2 Schematic form of the disk and the pad in sliding contact

$$E_c = \frac{1}{2}MV_0^2 \tag{1}$$

where M is the total mass of the vehicle and V_0 is the initial speed of the vehicle. To obtain the amount of heat dissipated by each of the front brake disks, we should know the weight distribution of the vehicle. So the amount of heat dissipated by each of the disks will be:

$$E = 0.5 \times \frac{1}{2}mV_0^2 = 0.25mV_0^2 \tag{2}$$

where m is the amount of the distributed mass on the front axle of the vehicle. Velocity of the vehicle slows down with the assumption of constant deceleration:

$$V = V_0\left(1 - {}^{t}/_{t_b}\right) \Rightarrow \omega = \omega_0\left(1 - {}^{t}/_{t_b}\right) \tag{3}$$

2.1.2 Microscopic model

Rate of generated heat due to friction is equal to the friction power. Some of this frictional heat is absorbed by the disk and the rest is absorbed by the pads. Two kinds of thermal contacts are usually used in analysis [21]:

(1) *Perfect contact*: considering the equal surface temperature of the disk and the pad.
(2) *Imperfect contact*: considering a heat resistance between the disk and the pad due to the formation of the third body constituted by detached particles. Where the imperfect contact is taken into account, the

heat partition coefficient is given by the following equation:

$$\sigma = \frac{\xi_d S_d}{\xi_d S_d + \xi_p S_p} \tag{4}$$

where ξ_p and ξ_d are the thermal effusivities of the pad and the disk and S_p and S_d are frictional contact surfaces of the pad and the disk, respectively. Thermal effusivity is defined as:

$$\zeta = \sqrt{k\rho c} \tag{5}$$

To calculate the frictional heat generation at the contact surfaces of two components of the brake system, parameters, e.g. the friction coefficient between two sliding components, relative sliding velocity, geometry of the disk brake rotor and the pad and the pressure distribution at the sliding surfaces must be available. Here two types of pressure distributions is considered:

2.1.2.1 Pressure distribution

- Uniform pressure

$$p = p_{\max} \tag{6}$$

- Uniform wear

$$\delta = kpr = \text{const} \Rightarrow p = p_{\max}\frac{r_2}{r} \tag{7}$$

where δ is wear, $p_{\max}$ is the maximum pressure distributed in the pad and p is the pressure at radial position r.

2.1.2.2 Heat generation Contact surface element of the pad and the disk is shown in Fig. 3. The rate of heat generated due to friction between these surfaces is calculated as follows:

$$\mathrm{d}\dot{E} = \mathrm{d}P = V\mathrm{d}F_f = r\omega\mu p\phi_0 r\mathrm{d}r \tag{8a}$$

$$\mathrm{d}\dot{E} = \mathrm{d}\dot{E}_p + \mathrm{d}\dot{E}_d \tag{8b}$$

$$\mathrm{d}\dot{E}_p = (1-\sigma)\mathrm{d}P = (1-\sigma)\mu p\omega\phi_0 r^2\mathrm{d}r \tag{8c}$$

$$\mathrm{d}\dot{E}_d = \sigma\mathrm{d}P = \sigma\mu p\omega\phi_0 r^2\mathrm{d}r \tag{8d}$$

where $\mathrm{d}\dot{E}$ is the rate of heat generated due to friction between two sliding components, V is the relative sliding velocity and $\mathrm{d}F_f$ is the friction force. The terms $\mathrm{d}\dot{E}_p$ and $\mathrm{d}\dot{E}_d$ are the amount of absorbed heat by the pad and the disk, respectively.

2.1.2.3 Heat flux To obtain the heat flux at the surfaces of two components of the brake system, we divide rate of thermal energy by the surface contact area of each component.

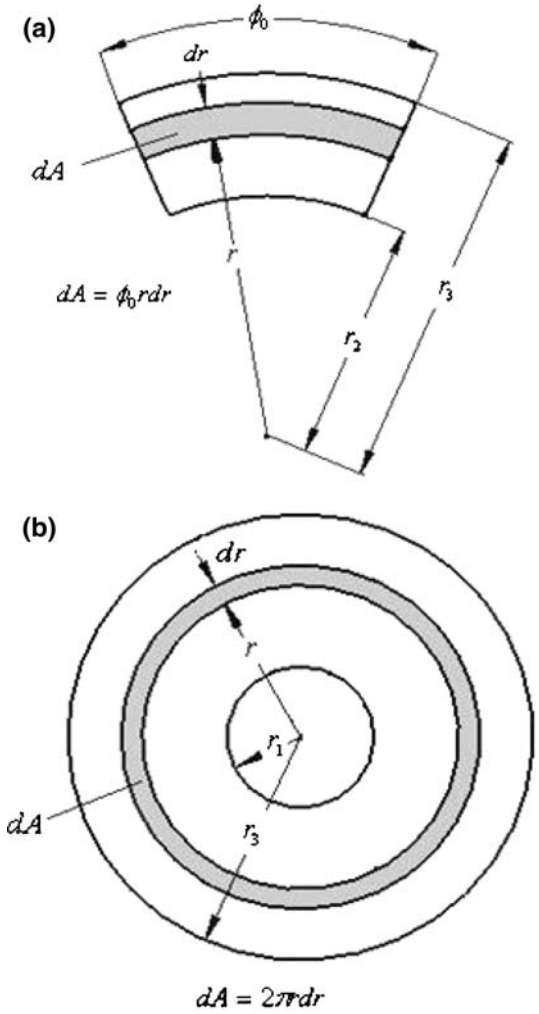

Fig. 3 Contact surface element of two components **a** the pad, **b** the disk

- Heat flux in the pad

$$q_1(r,t) = \frac{\mathrm{d}\dot{E}_p}{\mathrm{d}S_p} = (1-\sigma)\mu pr\omega(t) \tag{9a}$$

$$q_{0_1}(r) = q_1(r,0) = (1-\sigma)\mu pr\omega_0 \tag{9b}$$

- Heat flux in the disk

$$q_2(r,t) = \frac{\mathrm{d}\dot{E}_d}{\mathrm{d}S_d} = \frac{\phi_0}{2\pi}\sigma\mu pr\omega(t) \tag{10a}$$

$$q_{0_2}(r) = q_2(r,0) = \frac{\phi_0}{2\pi}\mu\sigma pr\omega_0 \tag{10b}$$

Heat flux for uniform pressure is a function of time and space variable r; the angular velocity decreases with time during braking action and the work done by friction force grows as radial space variable increases. This phenomenon is quite often when the pads are new. However after several braking, assumption of uniform wear is more realistic. Heat

flux obtained for the uniform wear is just a function of time and it is independent of the space variable; the work done by friction force is the same at radial direction.

3 Governing equation for two components in sliding contact

By looking at the mechanism of the disk brake, it may be deduced that we have temperature gradient in ϕ direction. On the other hand, since the disk is turning, the temperature gradient in ϕ direction is negligible. Also experimental investigations approve this phenomenon [4, 22]. So we can assume that the pad acts on the entire circumferential angle of the disk, so that the amount of generated heat is divided by this hypothetical surface. Hence the heat equation for the disk and the pad will be a function of r, z and t while independent of ϕ.

3.1 Hat equation for the pad

Figure 4 shows the two dimensional thermal problem of the pad. Heat equation and the appropriate boundary conditions for the pad may be written in the following form:

$$\frac{\partial^2 T}{\partial r^2}+\frac{1}{r}\frac{\partial T}{\partial r}+\frac{\partial^2 T}{\partial z^2}=\frac{1}{\alpha_p}\frac{\partial T}{\partial t};\quad r_2<r<r_3,\ \ 0<z<d_1,\ \ t>0 \tag{11a}$$

$$-\frac{\partial T}{\partial r}+H_{\mathrm{p}}T=H_{\mathrm{p}}T_\infty;\quad r=r_2,\ \ 0\le z\le d_1,\ \ t\ge 0 \tag{11b}$$

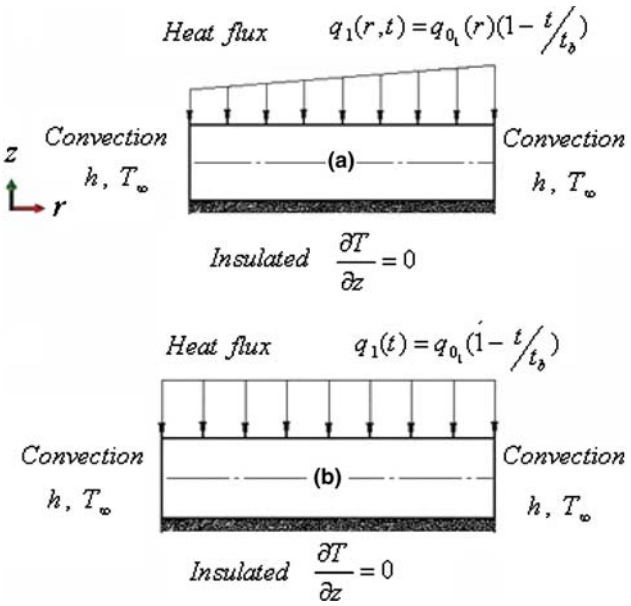

Fig. 4 Boundary conditions for the pad. **a** Uniform pressure, **b** uniform wear

$$\frac{\partial T}{\partial r}+H_{\mathrm{p}}T=H_{\mathrm{p}}T_\infty;\quad r=r_3,\ \ 0\le z\le d_1,\ \ t\ge 0 \tag{11c}$$

$$\frac{\partial T}{\partial z}=q_1(r,t);\quad z=0,\ \ r_2\le r\le r_3,\ \ t\ge 0 \tag{11d}$$

$$\frac{\partial T}{\partial z}=0;\quad z=d_1,\ \ r_2\le r\le r_3,\ \ t\ge 0 \tag{11e}$$

$$T(r,z,0)=f(r,z)=T_0;\quad r_2\le r\le r_3,\ \ 0\le z\le d_1 \tag{11f}$$

Parameter H_{p} is defined as:

$$H_{\mathrm{p}}=\frac{h}{k_{\mathrm{p}}} \tag{12}$$

The exact solution of this problem by use of Green's function approach, gives the following relationship for pad temperature [24]:

$$\begin{aligned}T_{\mathrm{p}}(r,z,t)=T_0\int_{r_2}^{r_3}\int_0^{d_1}G(r,z,t|r',z',0)r'\mathrm{d}r'\mathrm{d}z'\\+\alpha_{\mathrm{p}}H_{\mathrm{p}}T_\infty\int_0^t\int_0^{d_1}[G(r,z,t|r_2,z',\tau)\\+G(r,z,t|r_3,z',\tau)]\mathrm{d}z'\mathrm{d}\tau\\+\alpha_{\mathrm{p}}\int_0^t\int_{r_2}^{r_3}G(r,z,t|r',0,\tau)q_1(r',\tau)r'\mathrm{d}r'\mathrm{d}\tau\end{aligned} \tag{13}$$

where $G(r, z, t|r', z', \tau)$ denotes the Green's function of the problem that is given by the following relation:

$$\begin{aligned}&G(r,z,t|r',z',\tau)\\&=\left[\sum_{m=1}^{\infty}\frac{1}{N(\beta_m)N(\eta_0)}R_0(\beta_m,r')R_0(\beta_m,r)\mathrm{e}^{-\alpha_{\mathrm{p}}\beta_m^2(t-\tau)}\right]\\&+\left[\sum_{n=1}^{\infty}\sum_{m=1}^{\infty}\frac{1}{N(\beta_m)N(\eta_n)}R_0(\beta_m,r')\right.\\&\left.\times R_0(\beta_m,r)\cos\eta_n z'\cos\eta_n z\right]\mathrm{e}^{-\alpha_{\mathrm{p}}\lambda_{nm}^2(t-\tau)}\end{aligned} \tag{14}$$

where $R_0(\beta_m, r) = S_0J_0(\beta_m r) - V_0Y_0(\beta_m r)$ is the eigenfunction and β_m is the eigenvalue along radial direction. The eigenvalues β_m's are positive roots of the following equation:

$$S_0U_0-V_0W_0=0 \tag{15}$$

The parameters used are defined as:

$$S_0=\beta_m Y_0'(\beta_m r_3)+H_{\mathrm{p}}Y_0(\beta_m r_3) \tag{16a}$$

$$U_0=\beta_m J_0'(\beta_m r_2)-H_{\mathrm{p}}J_0(\beta_m r_2) \tag{16b}$$

$$V_0 = \beta_m J_0'(\beta_m r_3) + H_p J_0(\beta_m r_3) \tag{16c}$$

$$W_0 = \beta_m Y_0'(\beta_m r_2) - H_p Y_0(\beta_m r_2) \tag{16d}$$

$$B = H_p^2 + \beta_m^2 \tag{16e}$$

$$\frac{1}{N(\beta_m)} = \frac{\pi^2}{2}\frac{\beta_m^2 U_0^2}{B(U_0^2 - V_0^2)} \tag{16f}$$

η_n's the eigenvalues along z direction and the eigenfunctions along z direction are obtained as follows:

$$Z(\eta_n, z) = \begin{cases} \cos \eta_n z; & \eta_n \neq 0 \\ 1; & \eta_0 = 0 \end{cases} \tag{17}$$

Eigenvalues η_n's are the positive roots of the following equation:

$$\sin(\eta_n d_1) = 0 \Rightarrow \eta_n = \frac{n\pi}{d_1}(n = 0,\ 1,\ 2, \ldots) \tag{18}$$

The norm along z direction is obtained from the following relation:

$$\frac{1}{N(\eta_n)} = \begin{cases} \frac{2}{d_1}; & \eta_n \neq 0 \\ \frac{1}{d_1}; & \eta_0 = 0 \end{cases} \tag{19}$$

The parameter λ_{nm} is obtained from the following relation:

$$\lambda_{nm}^2 = \eta_n^2 + \beta_m^2; \quad \lambda_{0m}^2 = \eta_0^2 + \beta_m^2 = \beta_m^2 \tag{20}$$

3.2 Heat equation for the disk

As it can be seen in Fig. 5, since the thermal problem in the disk is symmetric in z direction, only the half of the disk ($z_2 = \frac{d_2}{2}$) is considered. So the transient heat equation for the disk and related boundary conditions that have been shown on Fig. 5 may be formulated as:

$$\frac{\partial^2 T}{\partial r^2} + \frac{1}{r}\frac{\partial T}{\partial r} + \frac{\partial^2 T}{\partial z^2} = \frac{1}{\alpha_d}\frac{\partial T}{\partial t}; \quad r_1 < r < r_3,\ 0 < z < z_2,\ t > 0$$

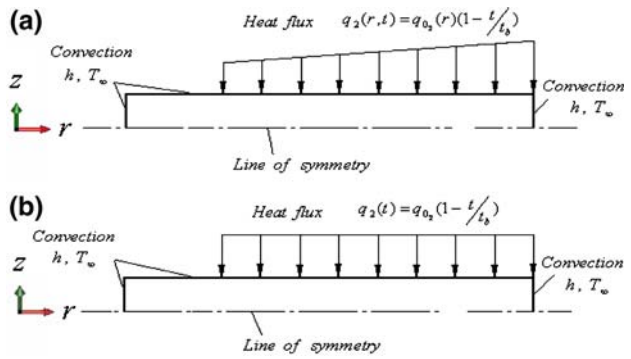

Fig. 5 Boundary conditions for the disk. **a** Uniform pressure, **b** uniform wear

$$-\frac{\partial T}{\partial r} + H_d T = H_d T_\infty; \quad r = r_1,\ 0 \le z \le z_2,\ t \ge 0$$

$$\frac{\partial T}{\partial r} + H_d T = H_d T_\infty; \quad r = r_3,\ 0 \le z \le z_2,\ t \ge 0$$

$$\frac{\partial T}{\partial z} = 0; \quad z = 0,\ r_1 \le r \le r_3,\ t \ge 0$$

$$\frac{\partial T}{\partial z} + H_d T = H_d T_\infty; \quad z = z_2,\ r_1 \le r \le r_2,\ t \ge 0$$

$$\frac{\partial T}{\partial z} = q_2(r,t); \quad z = z_2,\ r_2 \le r \le r_3,\ t \ge 0$$

$$T(r,z,0) = f(r,z) = T_0; \quad r_1 \le r \le r_3,\ 0 \le z \le d_2 \tag{21}$$

Parameter H_d is defined as:

$$H_d = \frac{h}{k_d} \tag{22}$$

Note that the heat generation has been considered as boundary condition of the second kind or prescribed heat flux boundary condition, as shown in Fig. 5. The exact solution of this problem by use of Green's function, gives the following relationship for disk temperature:

$$\begin{aligned} T_d(r,z,t) = {} & T_0 \int_{r_1}^{r_2}\int_0^{z_2} G_1(r,z,t|r',z',0)r'\mathrm{d}r'\mathrm{d}z' \\ & + T_0 \int_{r_2}^{r_3}\int_0^{z_2} G_2(r,z,t|r',z',0)r'\mathrm{d}r'\mathrm{d}z' \\ & + \alpha_d H T_\infty \int_0^t\int_0^{z_2} [G_1(r,z,t|r_1,z',\tau) \\ & + G_2(r,z,t|r_3,z',\tau)]\mathrm{d}z'\mathrm{d}\tau \\ & + \alpha_d H T_\infty \int_0^t\int_{r_1}^{r_2} G_1(r,z,t|r',z_2,\tau)r'\mathrm{d}r'\mathrm{d}\tau \\ & + \alpha_d \int_0^t\int_{r_2}^{r_3} G_2(r,z,t|r',z_2,\tau)q_2(r',\tau)r'\mathrm{d}r'\mathrm{d}\tau \end{aligned} \tag{23}$$

where $G(r, z, t|r', z', \tau)$ denotes Green's function of the problem that is given by the following relation:

$$G(r,z,t|r',z',\tau) = \begin{cases} G_1(r,z,t|r',z',\tau); & r_1 \le r \le r_2 \\ G_2(r,z,t|r',z',\tau); & r_2 \le r \le r_3 \end{cases} \tag{24}$$

where $G_1(r, z, t|r', z', \tau)$ and $G_2(r, z, t|r', z', \tau)$ are obtained from the following relations:

$$G_1(r,z,t|r',z',\tau) = \sum_{m=1}^{\infty}\sum_{n=1}^{\infty} A_1(m,r)B_1(n,z)\mathrm{e}^{-\alpha_d \lambda_{1,nm}^2 (t-\tau)} \tag{25a}$$

$$G_2(r,z,t|r',z',\tau) = \sum_{m=1}^{\infty} \frac{A_2(m,r)}{z_2} e^{-\alpha_d \beta_{2,m}^2 (t-\tau)} + \sum_{n=1}^{\infty}\sum_{m=1}^{\infty} A_2(m,r)B_2(n,z) e^{-\alpha_d \lambda_{2,nm}^2 (t-\tau)} \quad (25b)$$

where $A_1(m, r)$, $A_2(m, r)$, $B_1(n, z)$ and $B_2(n, z)$ are defined as:

$$A_1(m,r) = \frac{1}{N(\beta_{1,m})} R_1(\beta_{1,m}, r') R_1(\beta_{1,m}, r) \quad (26a)$$

$$A_2(m,r) = \frac{1}{N(\beta_{2,m})} R_2(\beta_{2,m}, r') R_2(\beta_{2,m}, r) \quad (26b)$$

$$B_1(n,z) = \frac{1}{N(\eta_{1,n})} Z_1(\eta_{1,n}, z') Z_1(\eta_{1,n}, z) \quad (26c)$$

$$B_2(n,z) = \frac{1}{N(\eta_{2,n})} Z_2(\eta_{2,n}, z') Z_2(\eta_{2,n}, z) \quad (26d)$$

The eigenvalues $\beta_{1,m}$ and $\beta_{2,m}$ are positive roots of the following equations:

$$\int_{r_1}^{r_2}\int_{0}^{z_2} r' G_1(r_2,z,t|r',z',0)\mathrm{d}z'\mathrm{d}r' = \int_{r_2}^{r_3}\int_{0}^{z_2} r' G_2(r_2,z,t|r',z',0)\mathrm{d}z'\mathrm{d}r' \quad (27a)$$

$$\int_{r_1}^{r_2}\int_{0}^{z_2} r' \frac{\partial G_1(r,z,t|r',z',0)}{\partial r}\bigg|_{r=r_2} \mathrm{d}z'\mathrm{d}r' = -\int_{r_2}^{r_3}\int_{0}^{z_2} r' \frac{\partial G_2(r,z,t|r',z',0)}{\partial r}\bigg|_{r=r_2} \mathrm{d}z'\mathrm{d}r' \quad (27b)$$

The eigenfunctions $R_1(\beta_{1,m}, r)$ and $R_2(\beta_{2,m}, r)$ are as follows:

$$R_1(\beta_{1,m}, r) = U_0 J_0(\beta_{1,m} r) - W_0 Y_0(\beta_{1,m} r) \quad (28)$$

$$R_2(\beta_{2,m}, r) = S_0 J_0(\beta_{2,m} r_3) - V_0 Y_0(\beta_{2,m} r_3) \quad (29)$$

where the parameters used are defined as:

$$U_0 = \beta_1 Y_0'(\beta_1 r_1) - H_d Y_0(\beta_1 r_1) \quad (30a)$$

$$W_0 = \beta_1 J_0'(\beta_1 r_1) - H_d J_0(\beta_1 r_1) \quad (30b)$$

$$V_0 = \beta_2 J_0'(\beta_2 r_3) + H_d J_0(\beta_2 r_3) \quad (30c)$$

$$S_0 = \beta_2 Y_0'(\beta_2 r_3) + H_d Y_0(\beta_2 r_3) \quad (30d)$$

The eigenfunctions $Z_1(\eta_{1,n}, z)$ $Z_2(\eta_{2,n}, z)$ are defined as follows:

$$Z_1(\eta_{1,n}, z) = \cos(\eta_{1,n} z) \quad (31)$$

$$Z_2(\eta_{2,n}, z) = \begin{cases} \cos(\eta_{2,n} z); & \eta_{2,n} \neq 0 \\ 1; & \eta_{2,0} = 0 \end{cases} \quad (32)$$

The eigenvalues $\eta_{1,n}$'s are the positive roots of the following equation:

$$\eta_{1,n} \tan(\eta_{1,n} z_2) = H_d \quad (33)$$

and the eigenvalues $\eta_{2,n}$'s are the positive roots of the following equation:

$$\sin(\eta_{2,n} z_2) = 0 \Rightarrow \eta_{2,n} = \frac{n\pi}{z_2}; \quad n = 0,\ 1,\ 2, \ldots \quad (34)$$

and the norms are obtained from the following relation:

$$\frac{1}{N(\eta_{1,n})} = \frac{2(\eta_{1,n}^2 + H^2)}{z_2(\eta_{1,n}^2 + H^2) + H} \quad (35)$$

$$\frac{1}{N(\eta_{2,n})} = \begin{cases} \frac{2}{z_2}; & \eta_{2,n} \neq 0 \\ \frac{1}{z_2}; & \eta_{2,0} = 0 \end{cases} \quad (36)$$

4 Automotive brake application

Consider the automotive disk brake issued from literature data. The details of the dimensions and operating conditions are given in Table 1. The disk material is steel while the pad material is made of an organic matrix composite. Their physical properties at room temperature are detailed in Table 2.

5 Results and discussion

Figure 6 shows the disk surface temperatures with respect to time. As it can be seen the current work results assuming uniform wear, are in a good agreement with Limpert and Newcomb models.

Maximum contact surface temperatures of the pad and the disk for two types of pressure distributions are illustrated in Fig. 7. Maximum temperature obtained for uniform pressure distribution is higher than that for uniform wear. The reason is that with the assumption of uniform pressure, the work done by friction force grows as the radius increases. Meanwhile the work done by friction force with the assumption of uniform wear does not vary with radius. Moreover the mean value of the surface temperature for the two pressure distribution is the same. As it can be seen, the difference between the surface temperature of the disk and the pad is relatively high. This is due to the thermal resistance between the disk and the pad, constituted by the accumulation of wear particles that form a thin layer (usually called third body). Therefore, this thermal resistance causes a heat partition between the disk and the pad.

Table 1 Parameters of automotive brake application [21]

Inner disk diameter	132 (mm)
Outer disk diameter	227 (mm)
Disk thickness	11 (mm)
Pad thickness	10 (mm)
Initial speed	100 (km h^{-1})
Braking time	3.96 (s)
Deceleration	7 (m s^{-2})
Total energy	165 (kJ)
Peak power time	0.5 (s)
Mean sliding radius	94.5 (mm)
Sliding length	37 (mm)
Convection coefficient	60 (W m^{-2} K^{-1})

Table 2 Parameters of automotive brake application [21]

Thermo-physical properties	Disk	Pad
Conductivity (W m^{-1} K^{-1})	43.5	12
Density (kg m^{-3})	7,850	2,500
Heat capacity (J kg^{-1} K^{-1})	445	900

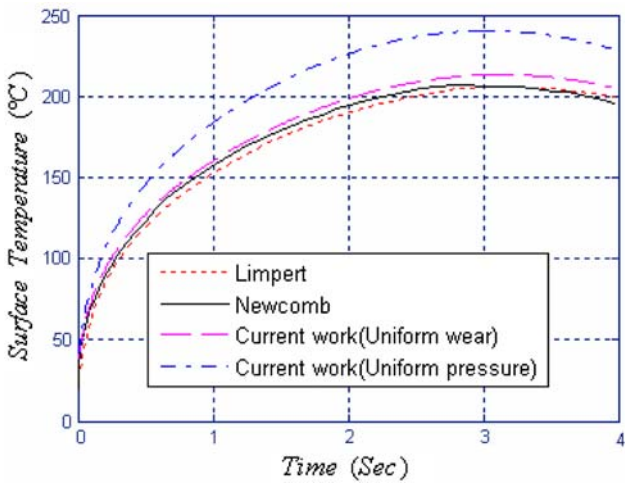

Fig. 6 Maximum disk surface temperature versus time

In Fig. 8 the pad surface temperature versus time, at different radial distances with the assumption of uniform pressure is illustrated. Every plot has a peak value at the time $t = 1.95$ s. At the beginning of the braking action the generated heat due to friction is very high and this frictional heat generation reduces gradually because, the relative sliding velocity between the pad and the disk decreases with time during the braking action. Therefore at the end of the braking action, the heat generation is equal to zero. It can be concluded that the maximum pad surface

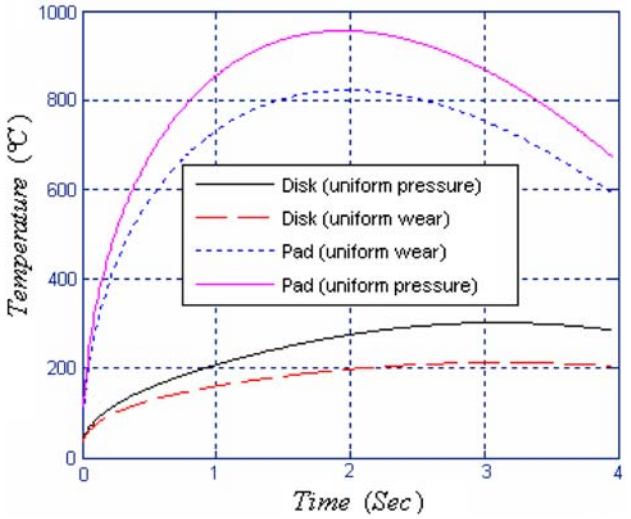

Fig. 7 Maximum disk and pad surface temperature versus time

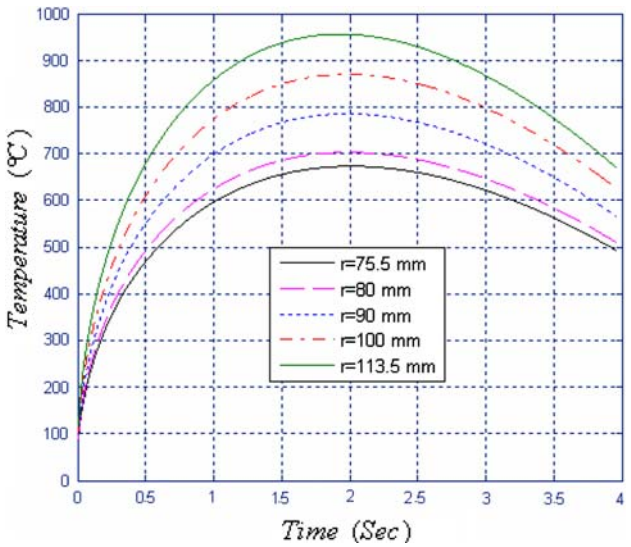

Fig. 8 Pad surface temperature at different radial distances (uniform pressure)

temperature is obtained almost at the middle of the braking time.

As it can be seen in Fig. 9 the pad temperature at the contact surface of the disk and the pad ($z = 0$) has the highest value and it gradually decreases at different axial locations up to $z = 10$ mm. Furthermore the slope $\frac{\partial T}{\partial t}\big|_{t=0}$ at the position of $z = 0$ has the highest value. Therefore at this point temperature increases with time rapidly. The slope decreases with time until the time $t = 1.95$ s that the slope is zero. This time is the time which maximum temperature occurs and after that the slope is negative and consequently temperature decreases with time. This behavior is dominant for $z = 2$ mm that maximum temperature is occurred at time $t = 3.06$ s and for $z = 4$ mm at

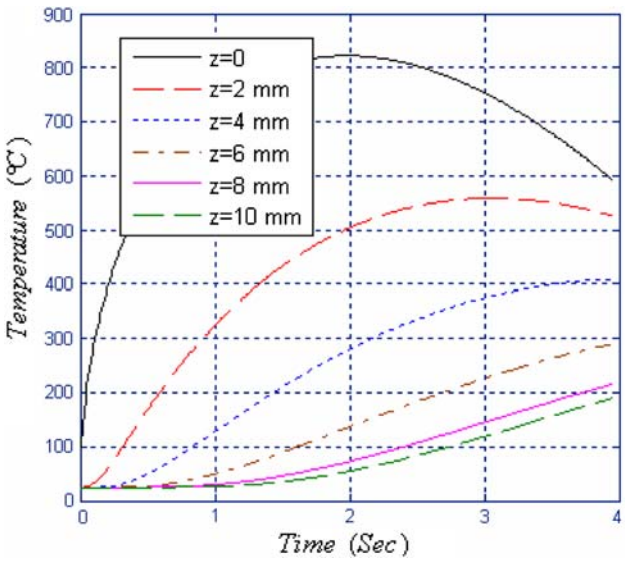

Fig. 9 Pad temperature at $r = 94.5$ mm and at different axial positions (uniform wear)

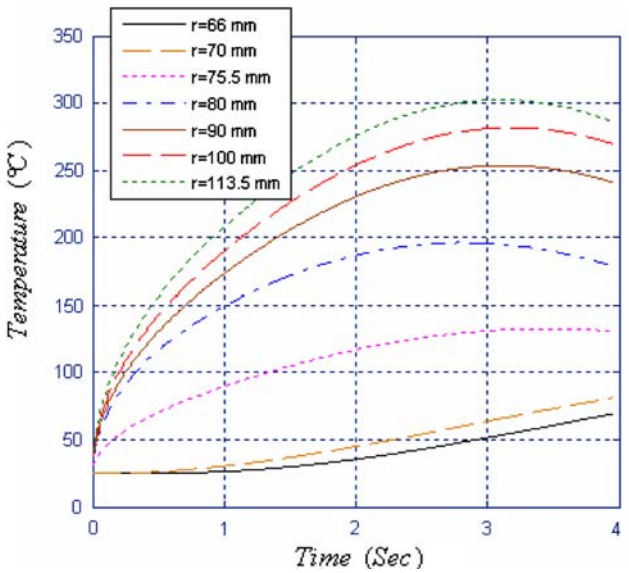

Fig. 10 Disk surface temperature at different radial distances (uniform pressure)

time $t = 3.96$ s. However at different axial position, e.g. $z = 6$, 8, 10 mm, this phenomenon is not dominant and the slope $\frac{\partial T}{\partial t}\big|_{t=0}$ decreases when z increases until $z = 10$ mm that the slope is equal to zero. At this position the slope increases with time which means the temperature is increasing with time. If the braking action is repeated, e.g. during mountain decent, this may be a concern, especially for the brake systems that equipped by aluminum calipers that may cause the brake fluid vaporization. On the other hand the highest value of the brake fluid temperature is often observed during the so-called heat soaking period or when the car is parked after long repetitive braking such as one which that may be encountered in a high mountain descent.

As it can be seen from Fig. 10 and as it is mentioned earlier the temperatures are increased in radial direction. The highest temperature occurs at the radial position of $r = 113.5$ mm and time of $t = 3.13$ s. As it can be seen, the slope $\frac{\partial T}{\partial t}$ of the plots at $r = 75.5$, 80, 90, 100, 113.5 mm, where the pad and the disk have sliding contact with each other, decreases with time and for the plots $r = 66$ and 70 mm, where the pad and the disk do not have any sliding contact, increases with time. This can be described by *Newton's law of cooling* which states that at the beginning of the braking action, temperatures of points that are closer to the friction surfaces increased with time, but after several seconds especially at the end of braking action and thereafter, temperature of points that are located at distant positions from friction surfaces increases rapidly.

As it can be seen from Fig. 11 the slope $\frac{\partial T}{\partial t}$ for the plots at radial positions of $r = 75.5$, 80, 94.5, 100, 113.5 mm,

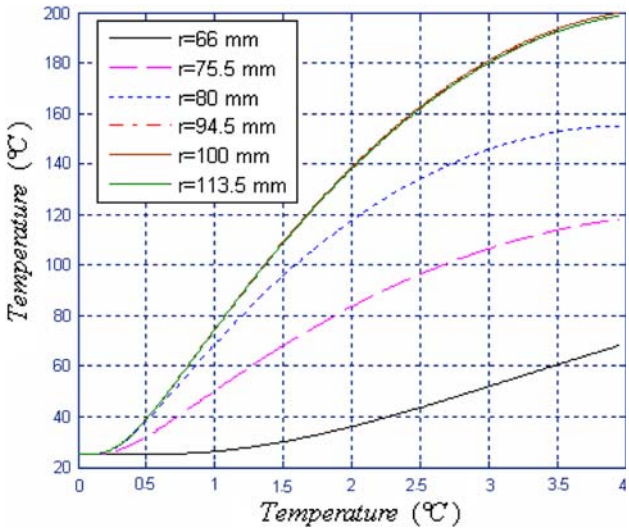

Fig. 11 Disk surface temperature at different radial distances (uniform wear)

where the pad and the disk have sliding contact with each other, decreases with time. Whereas, for the plot at $r = 66$ mm, where the pad and the disk do not have any sliding contact with each other, increases with time. This phenomenon is explained by *Newton's law of cooling* as mentioned earlier. However because of the assumption of uniform wear, the plots at $r = 94.5$, 100, 113.5 mm coincide with each other.

In Fig. 12 the disk temperature at the mean sliding radius and different axial positions with the assumption of uniform wear is illustrated. Here, because of symmetrical behavior along the axial direction, the position of $z = 0$ is

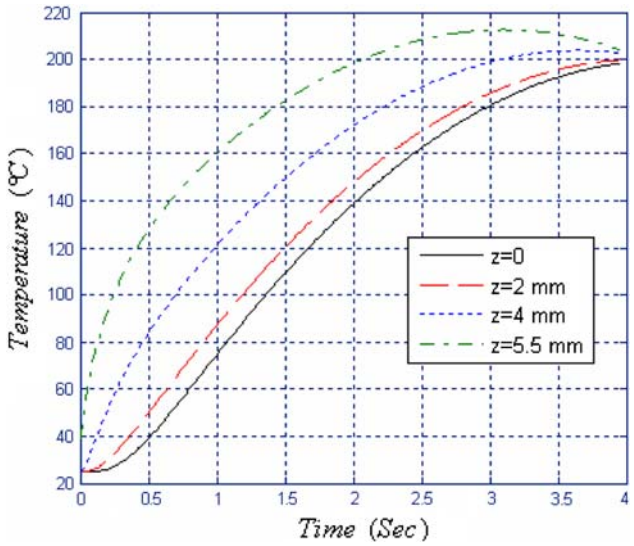

Fig. 12 Disk temperature at mean sliding radius and at different axial position (uniform wear)

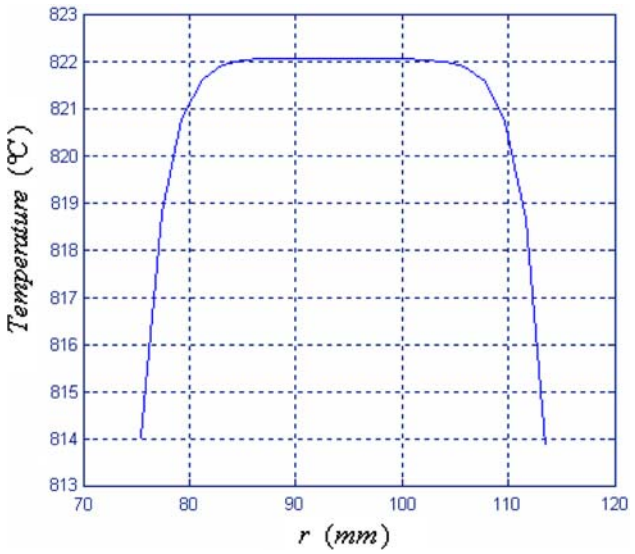

Fig. 13 Pad surface temperature difference in radial direction (uniform wear)

assumed as the line of symmetry. As it can be seen, at the beginning of the braking action, the temperature at the surface of the disk is higher than those for other axial positions. All of these diagrams at the end of the braking time merge which is an indication of the fact that the most quantity of the heat generated (about 93.4%) at the surface contact of the disk and the pad is absorbed by the disk. This absorbed heat should be dissipated to the environment through the disk and by means of heat convection.

In Fig. 13 the pad surface temperature in radial distances is illustrated. As it can be seen temperature difference between the highest and the lowest value in radial positions is as low as 8°C. This difference is because of the heat convection at the external boundaries at the radial positions of $r = r_2$ and $r = r_3$.

In Fig. 14 pad temperature in axial direction at the time of $t = 1.98$ s with the assumption of uniform wear is illustrated. As it can be seen, the value of the temperature differences in the axial direction is very high (about 767.54°C). However this temperature distribution is dominant for the time period that the pads have sliding contact with the disk. After this period especially when the car is parked, according to *Newton's law of cooling*, the temperature at the position of $z = 0$ decreases meanwhile the temperature at $z = 10$ mm increases rapidly, because of low convection coefficient (*natural convection*) and heat soaking phenomena.

In Fig. 15 pad temperature in axial direction at different radial distances and at the end of the braking time is illustrated. As it can be seen, the value of temperature difference in axial direction is relatively high. Furthermore,

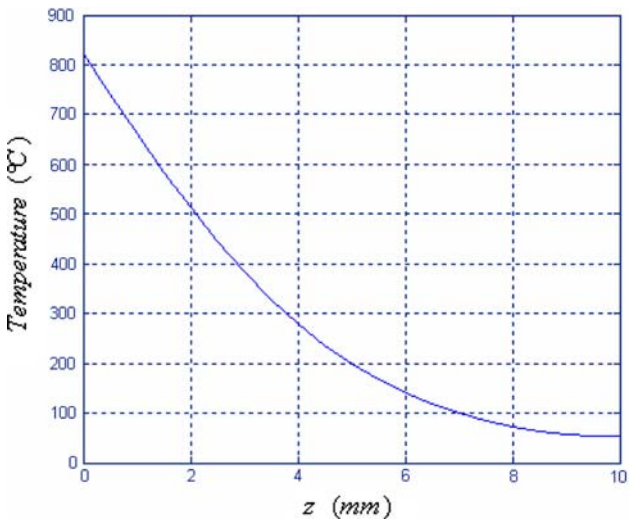

Fig. 14 Pad temperature in axial direction (uniform wear)

because of the assumption of uniform pressure, the temperature grows as the radial distance increases.

As it can be seen from Fig. 16 temperatures in radial distances have almost a linear behavior. Since, as mentioned earlier the work done by friction force for the assumption of uniform pressure is proportional to radial distance.

Figures 17 and 18 show the behavior of the disk temperature in radial and axial direction with the assumption of uniform wear. As it can be seen, the temperature variation in axial direction is not so high. The highest temperature difference in axial direction occurs at the contact zone

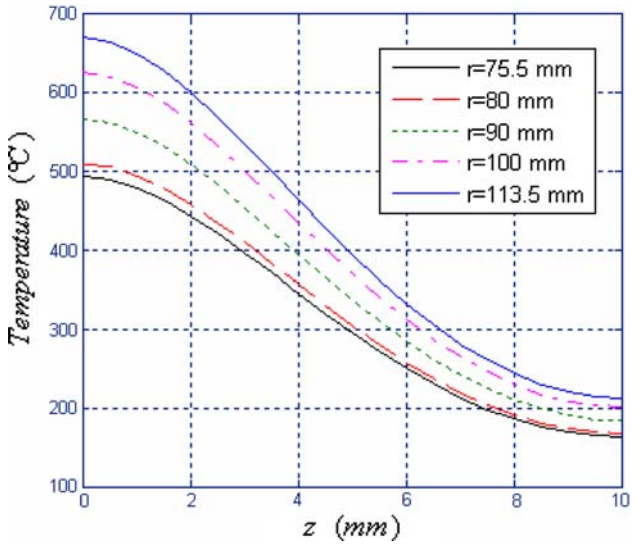

Fig. 15 Pad temperature in axial direction and at different radial distances (uniform pressure)

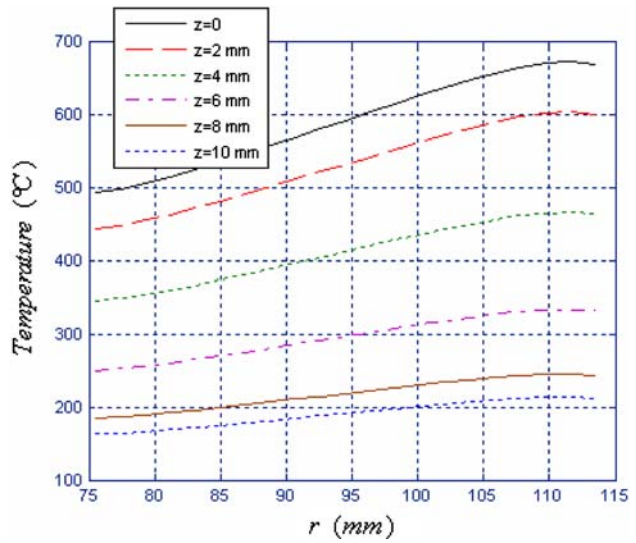

Fig. 16 Pad temperature in radial distances and at different axial positions (uniform pressure)

between $r = 75.5$ and $r = 90$ mm. The temperature difference in radial direction between $r = 66$ and $r = 90$ mm is very high, thereafter up to the position of $r = 113.5$ mm, there is no noticeable variation in temperature value.

Figures 19 and 20 show the behavior of disk temperature in radial and axial direction with the assumption of uniform pressure. As it can be seen, the temperature variation in axial direction is not noticeable. However, there is a temperature increase in radial direction because the work done by friction force grows as the radial distance increases.

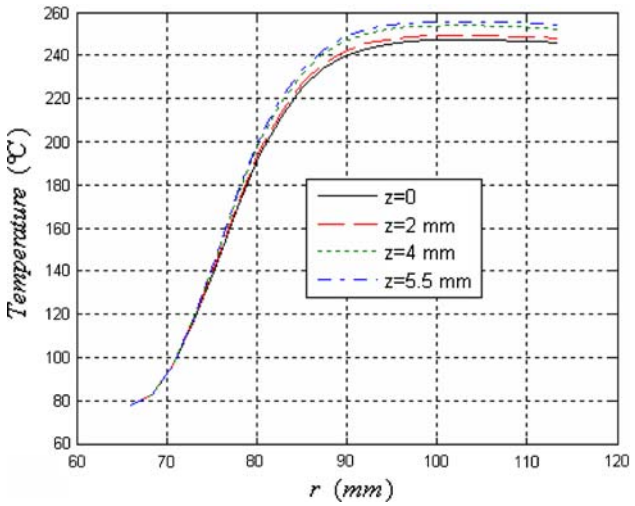

Fig. 17 Disk temperature in radial distances and at different axial positions (uniform wear)

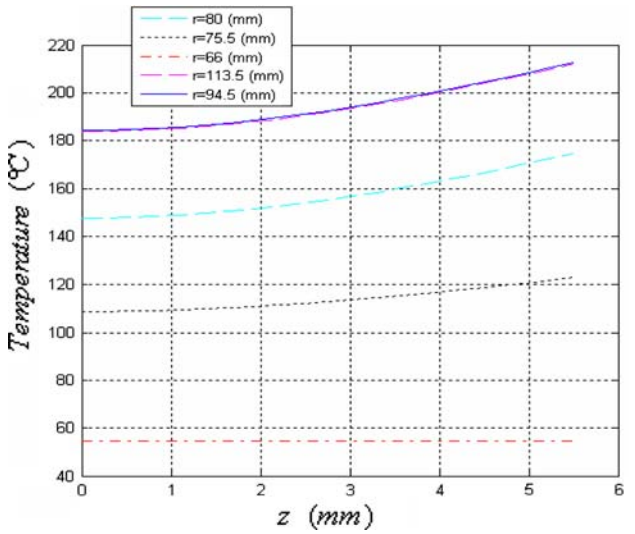

Fig. 18 Disk temperature in axial distances and at different radial positions (uniform wear)

In many studies [7, 21, 23] the heat generated due to friction was calculated using macroscopic model whereas, in this paper true representation of heat generation during braking action within the rotors and the pad, is investigated using macroscopic and microscopic model. Using microscopic model help us to better understand the effect of parameters such as the duration of braking, velocity of the vehicle and it's variation with time, dimensions and geometry of the brake system, material of the brake rotor and the pad and pressure distribution in the contact zone. Furthermore the heat flux calculated in these studies is considered only as a function of time. However, in this paper the heat flux calculated as a function of time and space variable.

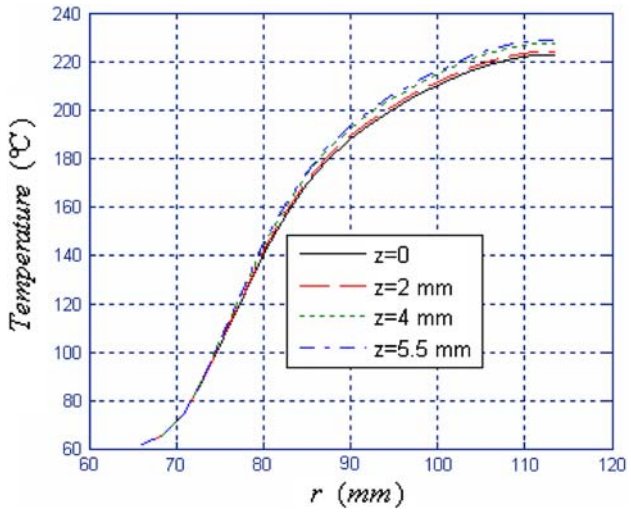

Fig. 19 Disk temperature in radial direction at different axial distances (uniform pressure)

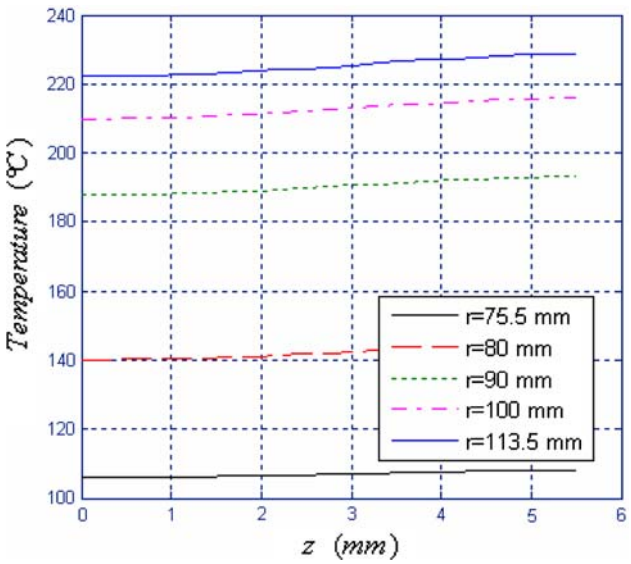

Fig. 20 Disk temperature in axial direction at different radial positions (uniform pressure)

6 Conclusion

The results obtained for contact surface temperatures of the pad and the disk show that there is a heat partition between two components in sliding contact, because of thermal resistance constituted by accumulation of wear particles at the contact surface between the pad and the disk and lack of necessary provisions for ventilation of the disk and heat dissipation to the environment through the disk.

In order to remove wear particles from contact zone of sliding components provisions are taken into account. One of these is to contrive slots on the surface of the pad (Fig. 21).

Fig. 21 Typical pads used for disk brake systems

Thermal resistance between the pad and the disk prevent the disk from absorbing the generated heat at the contact surface of the pad, so that temperature of the pad increases and consequently heat soaking to brake fluid increases and this may cause brake fluid vaporization. Therefore another provision that should be taken into account is to use a brake fluid with an appropriate *DOT rating* regarding to minimum dry and wet boiling points.

The brake rotor must serve as an efficient energy dissipation and storage device. In order to achieve this purpose, air must be circulated through the rotor to provide adequate cooling. The passages, formed by the radial fins between the braking surfaces, act as a centrifugal fan, facilitating the required air flow for cooling.

References

1. Lee K (1999) Numerical prediction of brake fluid temperature rise during braking and heat soaking. SAE, International Congress and Exposition Detroit, Michigan, 1–4 March. URL: http://delphi.com/pdf/techpapers/1999-01-0483.PDF
2. Valvano T, Lee K (2000) An analytical method to predict thermal distortion of a brake rotor. SAE, World Congress, Detroit, Michigan, 6–9 March. URL: http://www.sae.org/technical/papers/2000-01-0445
3. Mackin TJ, Noe SC et al (2002) Thermal cracking in disc brakes. Eng Failure Analysis 9(1):63–76. URL:http://www.ingentaconnect.com/content/els/13506307/2002/00000009/00000001/art00037
4. Yevtushenko A, Chapovska R (1997) Effect of time-dependent speed on frictional heat generation and wear in transient axisymmetrical contact of sliding. Arch Appl Mech 67:331–338. doi:10.1007/s004190050121
5. Ostermeyer GP (2001) On the dynamics of the friction coefficient. J Wear 254(9):852–858. doi:10.1016/S0043-1648(03)00235-7

6. Gao CH, Lin XZ (2002) Transient temperature field analysis of a brake in a non-axisymmetric three-dimensional model. J Mat Proc Tech 129:513–517. doi:10.1016/S0924-0136(02)00622-2
7. Dufrénoy P (2004) Two-/three-dimensional hybrid model of the thermomechanical behavior of disc brakes. J Rail Rapid Transit Part F 218:17–30. doi:10.1243/095440904322804402
8. Voldřich J (2006) Frictionally excited thermoelastic instability in disc brakes—Transient problem in the full contact regime. Int J Mech Sci 49(2):129–137. doi:10.1016/j.ijmecsci.2006.08.008
9. Naji M, Al-Nimr M, Masoud S (2000) Transient thermal behavior of a cylindrical brake system. J Heat Mass Transf 36:45–49
10. Mosleh M, Blau PJ, Dumitrescu D (2004) Characteristics and morphology of wear particles from laboratory testing of disk brake materials. J Wear 256:1128–1134. doi:10.1016/j.wear.2003.07.007
11. Mutlu I, Alma MH, Basturk MA (2005) Preparation and characterization of brake linings from modified tannin-phenol formaldehyde resin and asbestos-free fillers. J Mat Sci 40(11):3003–3005. doi:10.1007/s10853-005-2396-7
12. Hecht RL, Dinwiddie RB, Wang H (1999) The effect of graphite flake morphology on the thermal diffusivity of gray cast irons used for automotive brake discs. J Mat Sci 34(19):4775–4781. doi:10.1023/A:1004643322951
13. Gudmand-Høyer L, Bach A, Nielsen GT, Morgen P (1999) Tribological properties of automotive disc brakes with solid lubricants. J Wear 232(2):168–175. doi:10.1016/S0043-1648(99)00142-8
14. Uyyuru RK, Surappa MK, Brusethaug S (2007) Tribological behavior of Al–Si–SiCp composites/automobile brake pad system under dry sliding conditions. J Tribol Int 40(2):365–373. doi:10.1016/j.triboint.2005.10.012
15. Cho MH, Cho KH, Kim SJ, Kim DH, Jang H (2005) The role of transfer layers on friction characteristics in the sliding interface between friction materials against gray iron brake disks. Trib Lett 20(2):101–108. doi:10.1007/s11249-005-8299-6
16. Boz M, Kurt A (2007) The effect of Al2O3 on the friction performance of automotive brake friction materials. J Tribo Int 40(7):1161–1169. doi:10.1016/j.triboint.2006.12.004
17. Blau PJ, McLaughlin JC (2003) Effects of water films and sliding speed on the frictional behavior of truck disc brake material. Trib Int 36(10):709–715. doi:10.1016/S0301-679X(03)00026-4
18. McPhee AD, Johnson DA (2007) Experimental heat transfer and flow analysis of a vented brake rotor. Int J Thermal Sci 47(4):458–467. doi:10.1016/j.ijthermalsci.2007.03.006
19. Wallis L, Leonardi E, Milton B, Joseph P (2002) Air flow and heat transfer in ventilated disk brake rotors with diamond and tear-drop pillars. Numer Heat Transf Part A 41:643–655. URL: http://openurl.ingenta.com/content?genre=article&issn=1040-7782&volume=41&issue=6-7&spage=643&epage=655
20. Johnson DA, Sperandei BA, Gilbert R (2003) Analysis of the flow through a vented automotive brake rotor. J Fluids Eng 125:979–986. doi:10.1115/1.1624426
21. Majcherczak D, Dufrénoy P, Naït-Abdelaziz M (2005) Third body influence on thermal friction contact problems: application to braking. J Tribol 127:89–95. doi:10.1115/1.1757490
22. Majcherczak D, Dufrenoy P, Berthier Y (2007) Tribological, thermal and mechanical coupling aspects of the dry sliding contact. Tribol Int 40:834–843. doi:10.1016/j.triboint.2006.08.004
23. Gotowicki PF, Nigrelli V, Mariotti GV, Aleksendric D, Duboka C (2005) Numerical and experimental analysis of a Pegs-Wing ventilated disk brake rotor, with pads and cylinders. 10th EAEC European Automotive Congress, Serbia, Serbia and Montenegro, 30th May–1st June 2005, EAEC05YU-AS04. URL:http://www.atnet.it/lista/EAEC05YU-AS04.pdf
24. Ozisik MN (1993) Heat conduction, Chap 3 and 6, 2nd edn. John Wiley, New York